J. Biochem. **142,** 517–524 (2007)
doi:10.1093/jb/mvm158

Structural Evidence for Endocrine Disruptor Bisphenol A Binding to Human Nuclear Receptor ERRγ

Ayami Matsushima[1], Yoshimitsu Kakuta[2], Takamasa Teramoto[2], Takumi Koshiba[3], Xiaohui Liu[1], Hiroyuki Okada[1], Takatoshi Tokunaga[1], Shun-ichiro Kawabata[3], Makoto Kimura[2] and Yasuyuki Shimohigashi[1,*]

[1]Laboratory of Structure-Function Biochemistry, Department of Chemistry, Research-Education Centre of Risk Science, Faculty and Graduate School of Sciences; [2]Laboratory of Biochemistry, Department of Agricultural Chemistry, Faculty and Graduate School of Agriculture; and [3]Laboratory of Life Biochemistry, Department of Biological Science, Faculty of Sciences, Kyushu University, Fukuoka 812-8581, Japan

Received May 30, 2007; accepted July 25, 2007; published online August 30, 2007

Many lines of evidence reveal that bisphenol A (BPA) functions at very low doses as an endocrine disruptor. The human estrogen-related receptor γ (ERRγ) behaves as a constitutive activator of transcription, although the endogenous ligand is unknown. We have recently demonstrated that BPA binds strongly to ERRγ (K_D = 5.5 nM), but not to the estrogen receptor (ER). BPA preserves the ERRγ's basal constitutive activity, and protects the selective ER modulator 4-hydroxytamoxifen from its deactivation of ERRγ. In order to shed light on a molecular mechanism, we carried out the X-ray analysis of crystal structure of the ERRγ ligand-binding domain (LBD) complexed with BPA. BPA binds to the receptor cavity without changing any internal structures of the pocket of the ERRγ-LBD apo form. The hydrogen bonds of two phenol-hydroxyl groups, one with both Glu275 and Arg316, the other with Asn346, anchor BPA in the pocket, and surrounding hydrophobic bonds, especially with Tyr326, complete BPA's strong binding. Maintaining the 'activation helix' (helix 12) in an active conformation would as a result preserve receptor constitutive activity. Our results present the first evidence that the nuclear receptor forms complexes with the endocrine disruptor, providing detailed molecular insight into the interaction features.

Key words: binding assay, bisphenol A, estrogen-related receptor γ (ERRγ), nuclear receptor, X-ray crystal structure.

Abbreviations: BPA, bisphenol A; CBB, Coomassie brilliant blue; CHAPS, 3-[3-(cholamidopropyl)dimethylammonio]-1-propanesulfonic acid; DES, diethylstilbestrol; ER, estrogen receptor; ERR, estrogen-related receptor; ERE, estrogen response element; ERRE, ERR-response element; LBD, ligand-binding domain; MALDI-TOF, matrix-assisted laser desorption ionization time-of-flight; NR, nuclear receptor; 4-OHT, 4-hydroxytamoxifen; and PCR, polymerase chain reaction.

Bisphenol A (BPA), 2,2-bis(4-hydroxyphenyl)propane, has a symmetrical chemical structure of HO-C_6H_4-$C(CH_3)_2$-C_6H_4-OH. BPA is used mainly in the production of polycarbonate plastics and epoxy resins. Its worldwide manufacture is ~3.2 million metric tons per year. BPA had been acknowledged as an estrogenic chemical able to interact with human estrogen receptors (ERs) (*1*, *2*). In recent years, many lines of evidence reveal that BPA functions at its very low doses as an endocrine disruptor (*3*–*7*).

All of these so-called 'low-dose effects' of BPA have been explained as the output effects of steroid hormone receptor ERs (*8*). However, since BPA's binding to ER and hormonal activity is extremely weak, 1,000–10,000 times lower than for natural hormones, the intrinsic significance of low-dose effects has been intangible and obscure. BPA's low-dose effects have been peer-reviewed by the National Toxicology Program of the United States (*9*), and extensively reviewed by vom Saal and Hughes (*7*). The discrepancy on low-dose effects prompted us to enquire whether BPA may interact with nuclear receptors (NRs) other than ER, and as a BPA receptor we have recently identified the human estrogen-related receptor γ (ERRγ) (*10*).

The ERRγ belongs to the orphan subfamily of NRs (*11*), all members of which (ERRα, ERRβ and ERRγ) are closely related to ERs (*12*, *13*). ERRγ behaves as a constitutive activator of transcription, presumably with intrinsic roles in differentiation and maturation of the foetal brain. Although the endogenous ligand is unknown, we have shown that BPA binds strongly to ERRγ, but not to ER (*10*). BPA preserves the ERRγ's basal constitutive activity, and protects the selective ER modulator 4-hydroxytamoxifen (4-OHT) from its deactivation of ERRγ.

In order to explain such BPA's activities at the structural basis, we carried out the crystallization of the ERRγ ligand-binding domain (LBD) complexed with BPA. We here report the structure of the complex and shed light on a molecular mechanism between BPA and

*To whom correspondence should be addressed. Tel: +81-92-642-2584; Fax: +81-92-642-2584;
E-mail: shimoscc@mbox.nc.kyushu-u.ac.jp

ERRγ-LBD. This is the first straight evidence that the nuclear receptor forms a complex with the endocrine disruptor BPA. In the interaction with the receptor ERRγ, BPA was demonstrated to act as an inverse antagonist against 4-OHT's inverse agonist activity.

MATERIALS AND METHODS

Materials—3-[3-(Cholamidopropyl)dimethylammonio]-1-propanesulfonic acid (CHAPS), EDTA, HEPES and γ-globulin were obtained from Sigma (St Louis, MO, USA). Glycerol was from Nacalai Tesque (Kyoto), and all other chemicals used were of analytical grade and purchased from Wako (Osaka).

Methods—The concentration of nuclear receptor protein was estimated by the Bradford method (*14*) using the protein assay solution with Coomassie brilliant blue (CBB) (Nacalai Tesque). Mass spectra of proteins were measured on a mass spectrometer Voyager™ DE-PRO (PerSeptive Biosystems Inc., Framingham, MA, USA) using the matrix-assisted laser desorption ionization time-of-flight (MALDI-TOF) method.

Construction of Recombinant Plasmid—The cDNA fragment encoding human ERRγ-LBD (corresponding to amino acid residues 222–458) were generated by polymerase chain reaction (PCR) from kidney QUICK-Clone™ cDNA (Clonetech, Mountain View, CA, USA) using specific primers. The amplified product was cloned into the expression vector pGEX 6P-1 (Amersham Biosciences, Piscataway, NJ, USA) using *Eco*RI and *Xho*I restriction enzyme sites to express the product as a glutathione *S*-transferase (GST) fusion protein.

Site-directed Mutagenesis of ERRγ—The constructed plasmid were served as a template for Ala-substituted mutants. The PCR method was carried out to introduce the single-point mutations by using a series of overlapping sense and antisense primer pairs. The PCR fragments containing the E275A, M306A, L309A, R316A, Y326A, N346A and F435A mutations were cut with *Eco*RI and *Xho*I, and then subcloned into the expressing vector pGEX 6P-1.

Saturation Binding Assay—Saturation binding assay was conducted essentially as reported (*15*) at 4°C overnight to minimize degradation of the ligand receptor complex in a final volume of 100 μl of binding buffer [10 mM HEPES (pH 7.5), 50 mM NaCl, 2 mM $MgCl_2$, 1 mM EDTA, 2 mM CHAPS and 2 mg/ml γ-globulin]. GST-ERRγ-LBD of 30–3000 ng and [^{3}H]BPA (185 GBq/mmol, America Radiolabeled Chemicals Inc., St Louis, MO, USA) with or without addition of unlabelled BPA (final concentration of 10 μM) to quantify the non-specific binding. Free radio-ligand was removed by centrifugation (4°C, 10 min, 14,000 r.p.m.) or filtration after incubation with 100 μl of 1% dextran-coated charcoal (Sigma, St Louis, MO, USA) in PBS (pH 7.4) for 10 min at 4°C. Specific binding of [^{3}H]BPA was calculated by subtracting the non-specific binding from the total binding.

Protein Expression and Purification—GST fusion protein of the ERRγ-LBD was expressed by using *Escherichia coli* BL21 as described previously (*10*). Purification was carried out by using an affinity column of glutathione-sepharose 4B (Amersham Biosciences). GST was cleaved on the resin by using a specific enzyme, PreScission Protease (Amersham Biosciences), for 4 h at 4°C. After incubation, ERRγ-LBD was eluted and its concentration determined by the Bradford method using a CBB solution (*14*).

Crystallization of Protein Complex Followed by X-Ray Data Collection and Processing—Purified ERRγ-LBD was concentrated by ultrafiltration. Co-crystallization with a 3-fold molar excess of BPA was carried out with the hanging drop vapour diffusion method. The crystals used for data collection were from a drop of 2 μl of ERRγ-LBD solution mixed with BPA and 2 μl of reservoir solution (50 mM HEPES pH 7.5, 0.75 M sodium citrate and 5% glycerol). For data collection, crystals were transferred into a cryoprotectant solution containing 24% glycerol in reservoir solution, then mounted in a nylon loop and flash-frozen in a nitrogen stream at 100 K. X-ray diffraction data were collected at the beamline BL38B1, SPring-8 (Hyogo, Japan). The data were integrated and scaled using the HKL*2*000 package (*16*).

Structure Determination and Refinement—A monomer model of ERRγ-LBD/4-OHT (1S9Q) was used as a search molecule for molecular replacement using MOLREP (*17*) in CCP4 (*18*). The position of the monomer in the asymmetric unit was located and the structure refined at 1.6 Å using REFMAC5 (*19*) in CCP4. Manual adjustment and rebuilding of the model including BPA and water molecules were performed using the program Coot (*20*). The final model contained residues 232–458 of ERRγ, one BPA, three glycerol and 387 water molecules. Multiple conformers were applied to Lys236, Ser239, Ile249, Tyr250, Val278, Lys284, Ser290, Met298, Ser303, Ser319, Ser358, Ile382, Gln389, Asp393, Gln400, Asp401, Gln406, His407, Met419, Ser428, Gln433 and Leu454. The final model was validated with PROCHECK (*21*). Date collection and structure refinement statistics are summarized in Table 1.

Minimum-energy Calculations—For the energy calculations of the geometry optimization of BPA, the conventional Hartree–Fock (HF) method was used on a computer program Gaussian (v. 03) with the 6-31G(d, p) basis set.

RESULTS AND DISCUSSION

Dimeric Structure of ERRγ-LBD—The crystals usable for data collection were obtained from a ERRγ-LBD solution mixed with BPA in the following reservoir solution: 50 mM HEPES pH 7.5, 0.75 M sodium citrate and 5% glycerol. We solved the crystal structure of the resulting ERRγ-LBD in a complex with BPA at a resolution of 1.6 Å (space group $P4_12_12$) (Table 1). The ERRγ-LBD crystallized in homodimeric form using crystallographic 2-fold symmetry, indicating that BPA binding does not interfere with homodimer formation (Fig. 1A). Homodimer formation of the purified ERRγ-LBD is also observed by MALDI-TOF mass spectrometry (Fig. 2), in agreement with the reported homodimeric binding of ERRs to DNA (*22*). A BPA molecule in the complex with ERRγ-LBD is defined very well from its electron density (Fig. 1B).

Table 1. **Data collection and refinement statistics for X-ray crystal analysis of the ERRγ. LBD complexed with BPA.**

Data set	
Space group	$P4_12_12$
Unit cell parameters	$a = 64.05$ Å
	$b = 64.05$ Å
	$c = 136.87$
Data collection	
Beam line	SPring-8 BL38B1
Wavelength (Å)	1.0
Resolution range (Å)	28.06–1.60
Number of reflections	
Observed	433–326
Unique	36;414
R_{sym} [a,b]	0.058 (0.349)
I/σ (I)[a]	40.4 (8.2)
Completeness (%)	99.6
Refinement statistics	
Resolution range (Å)	28.06–1.60
Number of reflections	36,414
Working set	34,493
Test set	1,921
Completeness (%)	99.6
R_{cryst} [c] (%)	16.9
R_{free} [d] (%)	19.7
Root mean square deviations	
Bond length (Å)	0.012
Bond angles (°)	1.333
Average B-factor (Å^2)	
Protein	18.9
BPA	15.5
Glycerol	39.1
Water	35.3
Number of atoms	2,357
Protein	1,935
BPA	17
Glycerol	18
Water	387
Ramachandran analysis	
Most favoured (%)	94.8
Allowed (%)	5.2
Generously allowed (%)	0.0
Disallowed (%)	0.0

[a]Values in parentheses are for the highest resolution shell. [b]$R_{sym} = \sum(-\langle I\rangle)/\sum\langle I\rangle$, where I is the intensity measurement for a given reflaction and $\langle I\rangle$ is the average intensity for multiple measurements of this reflaction. [c]$R_{cryst} = \sum|F_{obs} - F_{cal}|\sum F_{obs}$, where F_{obs} and F_{cal} are observed and calculated structure factor amplitudes. [d]R_{free} value was calculated for R_{cryst}, using only an undefined subset of reflection data (5%).

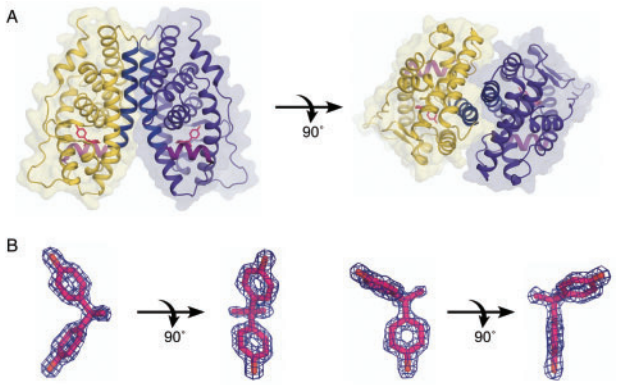

Fig. 1. **BPA/ERRγ-LBD complex.** (A) The panoramic view of whole-sphere BPA/ERRγ-LBD homodimer complex. Each panel shows the 3D-structure pictured from the top with 90° rotation. One molecule of BPA is in each ERRγ-LBD. BPA is shown in red colour. Characteristic α-helices are shown in distinctive colours; *i.e.* H10 in a dimerization interface, blue; H12 in an activation conformation, purple. (B) BPA bound to the ERRγ-LBD fitted into omitted Fo–Fc electron density maps at a level of 4.0 sigma. Right-side two panels show the aromatic face of BPA-A ring in a 90° rotation. Left-side two panels show the whole figure of the BPA molecule in a 90° rotation.

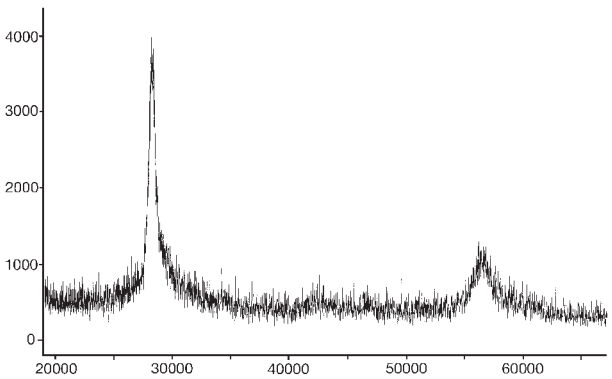

Fig. 2. **Dimer formation detected by MALDI-TOF mass spectrometry.** The peak of monomer emerges around 27,600 (calculated mass number [MH$^+$] of ERRγ-LBD: 27578.67), while the dimer peak is found at around 55,200.

ERRγ binds to the ERR-response element (ERRE), but as a monomer. ERRγ can also bind to functional estrogen response elements (EREs) in ER target genes, suggesting a possible overlap between ERR and ER action (*12*). Homodimers formed by the hydrophobic interactions between the interfaces of α-helix 10 (H10), which is supported by α-helix 7 (H7). Thus, in a homodimer, four α-helices are arranged in tandem to form the sequence H7–H10–H10–H7 (Fig. 1A, right). In the dimerization interface of H10–H10, such amino acid pairs as Pro422–*Pro422*, Arg425–*Gln426* and Gln426–*Arg425* appear to make a specific intermolecular interaction (Fig. 3A; the residues in italic characters are of the second molecule of ERRγ dimer). At the interface between H7 and H10, Tyr356–Thr420 and Met359–Met417 pairs are likely to underlie the intramolecular interaction (Fig. 3B). Leu418 and Leu421 in H10 are oriented towards the centre of the ERRγ-LBD and are conserved among almost all the NRs. In addition, almost all NRs conserve Leu399 in H9, and this Leu399 together with Leu418 and Leu421 in H10 take part in forming a hydrophobic core, which probably plays an intrinsic role in structural construction for homodimerization (Fig. 3C).

Binding Site of Bisphenol A—The binding site of BPA is constructed by a series of amino acid residues.

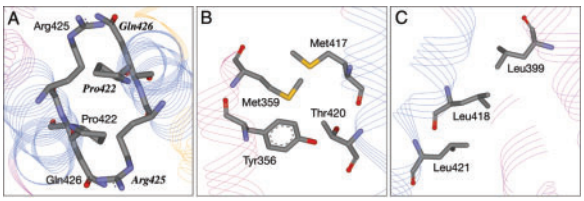

Fig. 3. **Intermolecular and intramolecular interactions of ERRγ-LBD.** (A) Dimer interface between H10 (blue) and *H10 (in the second molecule shown in italics)* is formed for amino acid residues such as Pro422–*Pro422*, Arg425–*Gln426*, and Gln426–*Arg425*. (B) Intramolecuar interaction between H7 (magenta) and H10 (blue) is seen for Tyr356 and Thr420, and for Met359 and Met417. (C) Highly conserved amino acid residues, Leu399 in H9, Leu418 and Leu421 in H10, are constructing a hydrophobic core.

Those in a range of 5 Å include Leu268, Cys269, Leu271, Ala272, Glu275 from H3; Trp305, Met306, Leu309, Val313, Arg316 from H5; Tyr326 from β-strand 1 (S1); Leu342, Leu345, Asn346, Ile349 from H7; Phe435 from H11 and Phe450 from H12 (Fig. 4A). In the BPA molecule, the two C_6H_4–OH (phenol) groups bind to the sp^3 carbon atom (sp^3-C) together with the two CH_3 groups, and thus their benzene-carbons adjacent to sp^3-C are arranged at the vertexes in a regular tetrahedron (Fig. 4B). It should be noted that BPA in the ERRγ-LBD complex is superimposed almost completely with BPA in the minimum-energy conformation (Fig. 4B). This demonstrates that BPA is present in the ERRγ-LBD binding pocket without any steric hindrance. Thus, BPA's phenol-hydroxyl oxygen atoms, C_6H_4–**O**H, are placed with a bond angle (O–sp^3–C–O) of about 105°, and are arranged to cross-link between Glu275/Arg316 and Asn346.

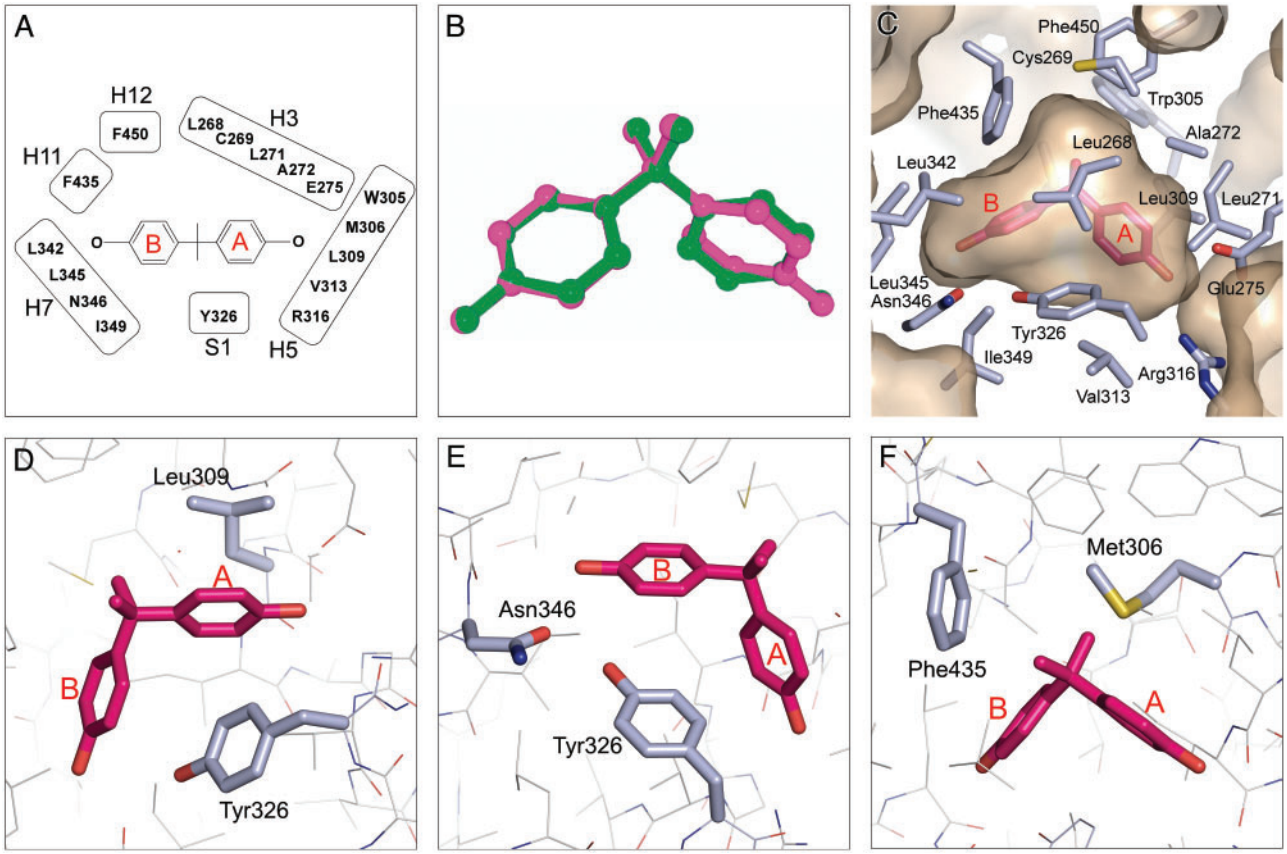

Fig. 4. **Identification of the binding sites of BPA in ERRγ-LBD.** (A) Schematic line-up of amino acid residues that form the LBP in ERRγ. The residues shown are in close proximity to BPA within 5 Å. (B) Superimposition of BPA (magenta) in the ERRγ-LBD complex and BPA (green) in the minimum-energy conformation calculated. They are almost completely overlaid, indicating that BPA fits the binding pocket of ERRγ-LBD without any conformational constrictions. The minimum-energy conformation was calculated and depicted by the conventional Hartree–Fock method using the computer program Gaussian (v. 03). (C) View of BPA in the cavity of ERRγ-LBD. The hydroxy groups of BPA's phenol-A and phenol-B rings are arranged to cross-link between Glu275/Arg316 and Asn346, respectively. (D) The BPA's A-ring is sandwiched with Leu309 and Tyr326 by characteristic hydrophobic interactions. The π face of A-ring interacts with the Leu309 isobutyl-methyl group, and the opposite π face of the same A-ring makes the T-shaped π/π interaction with Tyr326's phenol-benzene ring. (E) The BPA's B-ring is in a hydrogen bond with the Tyr326-phenol hydroxyl group. This OH/π bond appears to be a strong diving force to tether BPA in the ERRγ-LBP, together with the hydrogen bond between B-ring's hydroxy group and Asn346-β-carbonyl. (F) One of the CH_3 groups on the BPA's sp^3-C atom faces to Phe435 (H11) in a distance of 3.7 Å and another CH_3 group faces to the Met306 sulphur atom in a distance of 3.6 Å.

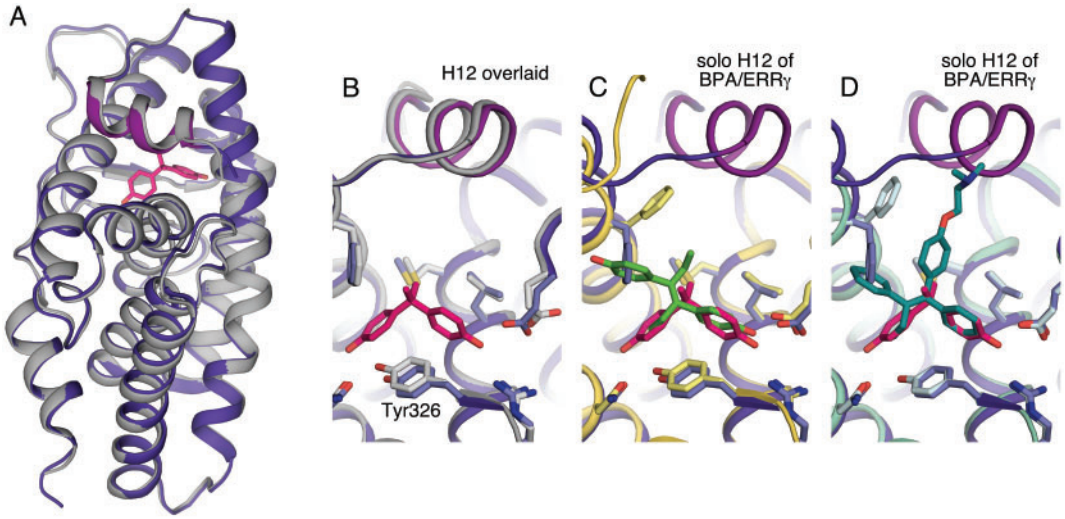

Fig. 5. **Superimposition of BPA or ERRγ-LBD and other ERRγ-LBD complexes.** (A) Superimposition of the whole LBD of BPA/ERRγ-LBD complex (blue) and the ERRγ-LBD apo form (grey) (1TFC; PDB code) (23). (B) The LBP of superimposed BPA/ERRγ-LBD complex (blue) and the ERRγ-LBD apo form (grey) (1TFC). The Tyr326-phenol groups are in a shift of about 10°, Tyr326-phenol of the BPA complex being underneath that of the apo form. (C) Superimposition of BPA/ERRγ-LBD complex (blue) and the DES/ERRγ-LBD complex (yellow) (1S9P) (23). The Tyr326-phenol groups are also in a slight shift. (D) Superimposition of the BPA/ERRγ-LBD complex (blue) and the 4-OHT/ERRγ-LBD (light blue) (1S9Q) (23). Superimposition of BPA (red) with DES (green) or 4-OHT (cyan) is carried out for α-helices to be overlaid. H12 in the BPA/ERRγ-LBD complex are shown in purple in all figures. H12 in the DES/ERRγ-LBD complex and in the 4-OHT/ERRγ-LBD complex are widely separated from a position in the activation conformation, and thus those are out of superimpositions between the BPA/ERRγ-LBD and the DES/ERRγ-LBD and 4–OHT/ERRγ-LBD complexes (C and D, respectively).

One of the two phenol-hydroxyl groups of BPA is anchored by hydrogen bonds with Glu275 (H3) and Arg316 (H5) at the one side of the ligand-binding pocket (LBP), while another hydroxyl group makes a hydrogen bond with Asn346 in H7 at the other side (Fig. 4C). Thus, BPA cross-links the residues Glu275/Arg316 and Asn346 with three hydrogen bonds. This is in stark contrast to the fact that diethylstilbestrol (DES) cross-links Glu275/Arg316 and His434 in H11 on the other side of the cavity (*23*). BPA's phenol-hydroxyl groups are not far enough apart to bridge between these Glu275/Arg316 and His434.

Key Amino Acid Tyr326 for Binding of Bisphenol A—Asn346 (H7) has been reported to interact with Tyr326 in S1 through a hydrogen bond (*23*, *24*). This hydrogen bond is also maintained in the BPA/ERRγ-LBD complex. In particular, we found that Tyr326 in the complex becomes the chief amino acid residue for BPA to be placed in the ERRγ-LBP, providing an appropriate and fitting space to pack BPA, having two phenol groups and two methyl groups. More importantly, Tyr326 interacts directly with BPA. The phenol group of the Tyr326 side chain keeps BPA's phenol-benzene rings A and B in the pocket by two strong interactions; i.e. by the hydrophobic *edge*-to-*face*-type, or T-shaped π/π interaction with BPA's benzene ring A, and by the OH/π interaction with BPA's benzene ring B (Fig. 4D and E). The Tyr-phenol benzene ring is able to make T-shaped π/π interactions with the aromatic side chains of amino acids such as Phe, Tyr, His and Trp (*25*, *26*). When one of six edges or vertexes of the benzene ring directs towards the π face of the counterpart aromatic ring, it makes so-called T-shaped π/π interaction(s). As seen in Fig. 4D, Tyr326's benzene ring indeed make a T-shaped π/π interaction with BPA's benzene ring A.

It should be noted that, at another π face on the opposite side, BPA's A ring interacts further with the Leu309 isobutyl-methyl groups (Fig. 4D). This interaction is also classified as a CH/π-type hydrophobic interaction. Consequently, there is a fascinating formation of sandwiched hydrophobic interactions of the A ring with Leu309 and Tyr326 (Fig. 4D). This is definitely a powerful driving force holding BPA in the LBD of ERRγ.

The Tyr326-phenol hydroxyl group makes another important interaction with BPA's benzene ring B. As shown in Fig. 4E, these are an OH/π interaction (*27*, *28*). OH/π interactions are one of the strongest interactions between amino acid side-chains (*25*, *26*). As a result, BPA's phenol B is tethered in the ERRγ-LBP complex by two essential interactions, the hydrogen bond with Asn346 and the OH/π bond with Tyr326.

It is noteworthy that Tyr326 has multiple interactions with BPA. In fact, Tyr326 might be in an ideal position to accept BPA in the ERRγ-LBP complex. When superimposition between ERRγ-LBD from the BPA/ERRγ-LBD complex and the ERRγ-LBD apo form (PDB code 1TFC) (*23*, *24*) was carefully checked, significant deviation was found for the Tyr326-phenol group (Fig. 5A and B). As shown in Fig. 5B, the Tyr326-phenol group in the BPA/ERRγ-LBD complex is pulled towards Asn346, shifting it through an angle of approximately 10°. This deviation keeps Tyr326-phenol group in the range of still stronger hydrogen bonds with Asn346, at a distance of 2.7 Å. All other amino acid residues in LBD are in exact agreement. In particular, the inside of the pocket is totally compatible with that of the apo form (Fig. 5A).

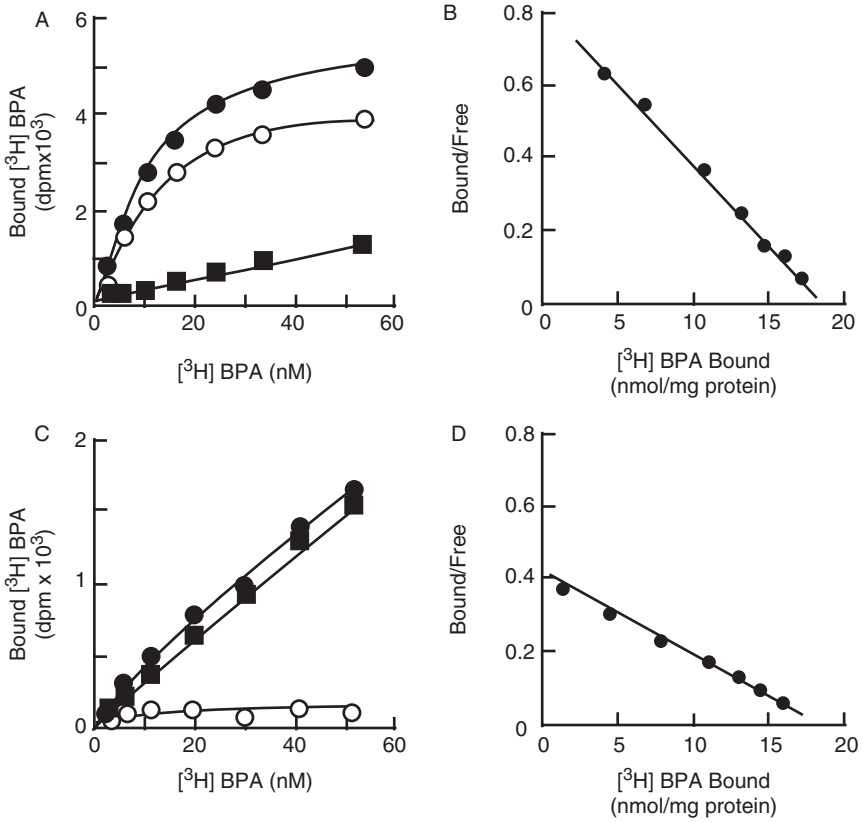

Fig. 6. **Receptor binding assays using tritium-labelled BPA.** (A) A sufficient specific binding of [^{3}H]BPA obtained in the saturation binding assay for wild-type ERRγ-LBD receptor. Closed circle, total binding; closed square, non-specific binding; and open circle, specific binding. (B) Scatchard plot analysis of [^{3}H]BPA for wild-type ERRγ-LBD. $K_D = 5.54 \pm 0.31$ nM, $B_{max} = 18.2 \pm 0.3$ nmol/mg protein. (C) No specific binding of [^{3}H]BPA shown in the saturation binding assay for ERRγ-LBD mutant receptor with E275A and R316A simultaneous substitutions. (D) Scatchard plot analysis of [^{3}H]BPA for ERRγ-LBD mutant receptor with N346A substitution. $K_D = 9.51 \pm 0.22$ nM, $B_{max} = 18.5 \pm 0.3$ nmol/mg protein. The Asn→Ala replacement was found to reduce approximately twice the dissociation constant, indicating that the Asn residue is important to the receptor binding of BPA presumably by the hydrogen-bonding between ERRγ-Asn-βCONH$_2$ and the BPA's phenol-hydroxyl group.

Interaction of Methyl Groups in Bisphenol A—BPA also has two methyl groups on the sp^3-C atom. One of these faces Phe435 (H11), and indeed the BPA-CH_3 and Phe435-phenyl groups are in close proximity (3.7 Å) to each other (Fig. 4F). On the other hand, another BPA-CH_3 group faces the Met306 sulphur atom with a non-covalent electron pair (3.6 Å between BPA-***C***H$_3$ and Met306-***S***) (Fig. 4F) making a form of electrostatic interaction. These interactions have been demonstrated by the drastically decreased binding activity that occurs in hexafluoro-BPA (designated as bisphenol AF), HO–C_6H_4–$C(CF_3)_2$–C_6H_4–OH, in which both CH_3 groups in BPA are replaced with trifluoromethyl CF_3 group. Electron-rich CF_3 would repel the electron-rich Phe-phenyl group and the Met-sulphur atom.

As mentioned earlier, BPA in the ERRγ-LBD complex is superimposed almost completely with BPA in the minimum-energy conformation (Fig. 4B). This implies that BPA fits spontaneously to the binding pocket of ERRγ-LBD without any conformational constraints, and binds specifically to each attachment position. It is likely that ERRγ possesses a binding pocket specifically adapted to the space requirements of the naturally occurring BPA-like ligand.

Superimposition of Bisphenol A/ERRγ-LBD Complex with Other Complexes—Superimposition of BPA and DES (1S9P) (*23*) in the ERRγ-LBD complexes shows conformational differences that can readily account for the differences in binding modes to the binding pocket. The phenol A ring of BPA superimposes almost completely with the corresponding A ring of DES, whereas the B rings orient in completely different directions (Fig. 5C). As a result, the phenol B ring of BPA heads towards H7 to capture Asn346 by its hydrogen bond, while that of DES goes towards H11 to restrain His434 also by a hydrogen bond.

Superimposition of the BPA complex and the 4-OHT complex (1S9Q) (*23*) of ERRγ-LBD, on the other hand, shows structural differences that make clear the difference in their activity mediated through the ERRγ. As before, the phenol A ring of BPA superimposes almost completely with the corresponding A ring of 4-OHT (Fig. 5D). Incontrast, the aromatic B ring of 4-OHT goes towards H11 with no hydrogen bond. The aromatic C ring of 4-OHT directs itself towards H12.

Greschik *et al.* (*23*) have reported that the binding of DES and 4-OHT to ERRγ-LBD dissociates the H12 region from the LBD body. DES- and 4-OHT-mediated

activities were explained by the three-dimensional structure of the DES/or 4-OHT/ERRγ-LBD complex, in which helix 12 is widely separated from a position in the activation conformation. Indeed, their H12s are out of superimpositions between the BPA/ERRγ-LBD and the DES/ or 4–OHT/ERRγ-LBD complexes (Fig. 5C and D). This repositioning of H12 by DES and 4-OHT deactivates ERRγ, because the receptor becomes unable to recruit coactivator proteins at the appropriate position. The LBD structure of ERRγ apo form has also been solved (*23*, *24*), and as expected from its very high constitutive activity, H12 of this non-liganded ERRγ-LBD is folded in the activation conformation (Fig. 5A).

Bisphenol A Holds ERRγ-LBD in the Activation Conformation—One of the most important findings in the present study is that H12 in the BPA/ERRγ-LBD complex is in the transcriptionally active conformation. H12 is associated firmly with the LBD body, where the coactivator binds. When we compared this crystal structure with the reported crystal structure (1TFC) of the apo form of ERRγ-LBD (*23*), almost no conformational changes were shown for almost all the atoms including both the main and side chains from H1 to H12 (Fig. 5A). Superimposition of the ERRγ-LBD from the BPA/ERRγ-LBD complex and the apo ERRγ-LBD shows their exact and entire agreement. In particular, the positioning and conformation of H12 is totally compatible with that of the apo form (Fig. 5A and B). Although H12's activation conformation in the apo form appeared to be maintained by the presence of a peptide derived from the coactivator protein SRC-1, H12 in the BPA/ERRγ-LBD complex is in fact in the activation conformation without the SRC-1 peptide.

These conformational consequences verify the high functional activity of BPA. ERRγ *per se* elicits a very high basal activity in the luciferase reporter gene assay. BPA was found to maintain this high spontaneous constitutive activity in ERRγ for a range of concentrations from 10^{-10} to 10^{-5} M BPA (*10*). Furthermore, BPA reverses the deactivation activity of 4-OHT, indicating that BPA displaces 4-OHT and repositions the H12 from the transcriptionally inactive conformation to the active conformation. It should be noted that the compounds that deactivate the receptor are termed as 'inverse agonist,' whereas those that inhibit such inverse agonists are defined as 'inverse antagonist.' Thus, BPA indeed acts as an inverse antagonist against the inverse agonist 4-OHT in ERRγ.

Structural Demonstration of the Binding Sites by Site-directed Mutagenesis—The amino acid residues in the BPA-binding site of ERRγ-LBD were substituted with Ala by means of the site-directed mutagenesis. Those included Glu275, Met306, Leu309, Arg316, Tyr326, Asn346 and Phe435 in the binding pocket. The resulting mutant receptors were examined by the saturation binding assay using tritium-labelled BPA (Fig. 6A and B). When Glu275 and Arg316 were substituted simultaneously, the mutant receptor exhibited almost no specific binding (Fig. 6C), indicating that these residues are critically important to bind BPA to the pocket. In contrast, [^{3}H]BPA was found to bind to Asn346Ala mutant receptor (B_{max} = 18.5 nmol/mg) as well as wild-type receptor (18.2 nmol/mg), although its binding affinity for the mutant was approximately 2-fold weaker (K_D = 9.51 nM) than that for the wild-type (5.54 nM) (Fig. 6D). All other mutant receptors exhibited considerably reduced specific binding and drastically weakened binding ability (10–20-fold larger K_D values). The results clearly evidenced that the structural elements complementary to BPA are indeed its binding sites.

Conclusion and Perspectives—The present study clearly indicates that the nuclear receptor ERRγ possesses a space in its LBD to which BPA can bind highly specifically and selectively. It is still not clear whether, under physiological conditions, ERRγ can function without an endogenous ligand, nor what ERRγ's physiological functions may be. The results we present imply that ERRγ may in fact have a BPA-like endogenous ligand, and will facilitate the design of novel specific agonist and antagonist compounds.

The binding affinity of [^{3}H]BPA to ERRγ-LBD is extremely high, with a K_D value of 5.5 nM. Thus, it is an immediate and important requirement to evaluate whether the previously reported effects of BPA at low doses are mediated through ERRγ and its specific target gene(s). At the same time, it is necessary to clarify what the physiological roles of ERRγ are, and to examine the extent of, and direction in which, BPA may influence these. This is particularly important because ERRγ is expressed in a tissue-restricted manner, for example, very strongly in the mammalian foetal brain and also in the placenta, at sites that could have important outcomes for the newborn.

We thank Prof. Ian A. Meinertzhagen, Dalhousie University, Canada, for reading the manuscript. This study was supported by Health and Labour Sciences Research Grants to Y.S., for Research on Risk of Chemical Substances, from the Ministry of Health, Labor and Welfare of Japan. This work was also supported in part by grants-in-aid from the Ministry of Education, Culture, Sports, Science and Technology of Japan to Y.S. We thank the staff of the SPring-8 BL38B1 beamline for help with the X-ray diffraction experiments. The work was supported by a grant for the National Project on Protein Structural and Functional Analyses from the Ministry of Education, Culture, Sports, Science and Technology of Japan. Atomic coordinates for the structure have been deposited in the Protein Data Bank with accession code 2E2R.

REFERENCES

1. Krishnan, A.V., Stathis, P., Permuth, S.F., Tokes, L., and Feldman, D. (1993) Bisphenol-A: an estrogenic substance is released from polycarbonate flasks during autoclaving. *Endocrinology* **132**, 2279–2286
2. Olea, N., Pulgar, R., Pérez, P., Olea-Serrano, F., Rivas, A., Novillo-Fertrell, A., Pedraza, V., Soto, A.M., and Sonnenschein, C. (1996) Estrogenicity of resin-based composites and sealants used in dentistry. *Environ. Health Perspect.* **104**, 298–305
3. Nagel, S.C., vom Saal, F.S., Thayer, K.A., Dhar, M.G., Boechler, M., and Welshons, W.V. (1997) Relative binding affinity-serum modified access (RBA-SMA) assay predicts the relative *in vivo* bioactivity of the xenoestrogens

bisphenol A and octylphenol. *Environ. Health Perspect.* **105**, 70–76
4. Markey, C.M., Luque, E.H., de Toro, M.M., Sonnenschein, C., and Soto, A.M. (2001) In utero exposure to bisphenol A alters the development and tissue organization of the mouse mammary gland. *Biol. Reprod.* **65**, 1215–1223
5. Kubo, K., Arai, O., Omura, M., Watanabe, R., Ogata, R., and Aou, S. (2003) Low dose effects of bisphenol A on sexual differentiation of the brain and behavior in rats. *Neurosci. Res.* **45**, 345–356
6. Kawai, K., Nozaki, T., Nishikata, H., Aou, S., Takii, M., and Kubo, C. (2003) Aggressive behavior and serum testosterone concentration during the maturation process of male mice: the effects of fetal exposure to bisphenol A. *Environ. Health Perspect.* **111**, 175–178
7. vom Saal, F.S. and Hughes, C. (2005) An extensive new literature concerning low-dose effects of bisphenol A shows the need for a new risk assessment. *Environ. Health Perspect.* **113**, 926–933
8. Welshons, W.V., Thayer, K.A., Judy, B.M., Taylor, J.A., Curran, E.M., and vom Saal, F.S. (2003) Large effects from small exposures. I. Mechanisms for endocrine-disrupting chemicals with estrogenic activity. *Environ. Health Perspect.* **111**, 994–1006
9. National Toxicology Program (NTP). U.S. Department of Health and Human Services, National Institute of Environmental Health Sciences, National Institute of Health. National Toxicology Program's Report of Endocrine Disruptors Low-Dose Peer Review (2001). Available on the NTP web site: http://ntp-server.niehs.nih.gov/htdocs/liason/LowDoseWebPage.html.
10. Takayanagi, S., Tokunaga, T., Liu, X., Okada, H., Matsushima, A., and Shimohigashi, Y. (2006) Endocrine disruptor bisphenol A strongly binds to human estrogen-related receptor γ(ERRγ) with high constitutive activity. *Toxicol. lett.* **167**, 95–105
11. Eudy, J.D., Yao, S., Weston, M.D., Ma-Edmonds, M., Talmadge, C.B., Cheng, J.J., Kimberling, W.J., and Sumegi, J. (1998) Isolation of a gene encoding a novel member of the nuclear receptor superfamily from the critical region of Usher syndrome type IIa at 1q41. *Genomics* **50**, 382–384
12. Giguère, V. (2002) To ERR in the estrogen pathway. *Trends Endocrinol. Metab.* **13**, 220–225
13. Horard, B. and Vanacker, J.M. (2003) Estrogen receptor-related receptors: orphan receptors desperately seeking a ligand. *J. Mol. Endocrinol.* **31**, 349–357
14. Bradford, M.M. (1976) A rapid and sensitive method for the quantitation of microgram quantities of protein utilizing the principle of protein-dye binding. *Anal. Biochem.* **72**, 248–254
15. Nakai, M., Tabira, Y., Asai, D., Yakabe, Y., Shimyozu, T., Noguchi, M., Takatsuki, M., and Shimohigashi, Y. (1999) Binding characteristics of dialkyl phthalates for the estrogen receptor. *Biochem. Biophys. Res. Commun.* **254**, 311–314
16. Otwinowski, Z. and Minor, W. (1997) Processing of X-ray diffraction data collected in oscillation mode. *Method Enzymol.* **276**, 307–326
17. Vagin, A. and Teplyakov, A. (1997) MOLREP: an automated program for molecular replacement. *J. Appl. Cryst.* **30**, 1022–1025
18. Collaborative Computational Project (1994) The CCP4 Suite: programs for protein crystallography. *Acta Cryltallogr. Sect. D Biol. Crystallogr.* **50**, 760–763
19. Murshudov, G.N., Vagin, A.A., and Dodson, E.J. (1997) Refinement of macromolecular structures by the maximum-likelihood method. *Acta Crystallogr. D Biol. Crystallogr.* **53**, 240–255
20. Emsley, P. and Cowtan, K. (2004) Coot: model-building tools for molecular graphics. *Acta Crystallogr. D Biol. Crystallogr.* **60**, 2126–2132
21. Laskowski, R.A., McArthur, M.W., Moss, D.S., and Thornton, J.M. (1993) A program to check the stereochemical quality of protein structures. *J. Appl. Cryst.* **26**, 283–291
22. Huppunen, J. and Aarnisalo, P. (2004) Dimerization modulates the activity of the orphan nuclear receptor ERR γ. *Biochem. Biophys. Res. Commun.* **314**, 964–970
23. Greschik, H., Flaig, R., Renaud, J.P., and Moras, D. (2004) Structural basis for the deactivation of the estrogen-related receptor γ by diethylstilbestrol or 4-hydroxytamoxifen and determinants of selectivity. *J. Biol. Chem.* **279**, 33639–33646
24. Greschik, H., Wurtz, J.M., Sanglier, S., Bourguet, W., van Dorsselaer, A., Moras, D., and Renaud, J.P. (2002) Structural and functional evidence for ligand-independent transcriptional activation by the estrogen-related receptor 3. *Mol. Cell* **9**, 303–313
25. Nishio, M., Umezawa, Y., Hirota, M., and Takeuchi, Y. (1995) The CH/π interaction: Significance in molecular recognition. *Tetrahedron* **51**, 8665–8701
26. Umezawa, Y. and Nishio, M. (2005) CH/π hydrogen bonds as evidenced in the substrate specificity of acetylcholine esterase. *Biopolymers* **79**, 248–258
27. Ôki, M. and Iwamura, H. (1967) Steric effects on the O – H $\cdots$ π interaction in 2-hydroxybiphenyl. *J. Am. Chem. Soc.* **89**, 576–579
28. Subramanian, S. and Zaworotko, M.J. (1994) Exploitation of the hydrogen bond: Recent developments in the context of crystal engineering. *Coordin. Chem. Rev.* **137**, 357–401